Supporting Information

Two photoluminscent metal-organic frameworks based on a BODIPY-derived bipyridine ligand

Lian Zhou,[a,b] Yun-Shan Xue,[a] Yan Xu,[c] Jun Zhang,[d] Hong-Bin Du[a,*]

[a] *State Key Laboratory of Coordination Chemistry, School of Chemistry and Chemical Engineering, Nanjing University, Nanjing, 210093, China. Fax: +86-25-83314502, E-mail:hbdu@nju.edu.cn.*

[b] *School of Chemical Engineering, Qinghai University, Xining, Qinghai,810006, China.*

[c] *Department of Chemistry, Nanjing University of Technology, Nanjing 210009.*

[d] *School of Materials and Chemical Engineering, Anhui University of Architecture, Hefei, 230601, China.*

Content

1- Selected bond lengths and angles of MOFs 1-2

Table S1 Selected bond lengths (Å) and angles (º) for **1**.

Zn1—O1W	1.938(5)	Zn2—O2	1.939(2)
Zn1—O3^{i}	2.025(2)	Zn2—N1	2.026(5)
Zn2—N2^{vi}	2.027(5)		
O1W—Zn1—O3^{i}	100.39(7)	O3^{i}—Zn1—O3^{ii}	88.14(2)
O3^{i}—Zn1—O3	159.22(14)	O3^{ii}—Zn1—O3	88.14(2)
O2—Zn2—O2^{v}	103.50(15)	O2—Zn2—N1	111.72(12)
O2—Zn2—N2^{vi}	111.67(12)	N1—Zn2—N2^{vi}	106.7(2)

Symmetry codes: (i) -x, -y, z; (ii) y, -x, z; (iii) -y, x, z; (iv) -x, -y, -z; (v) x, y, 1-z; (vi) 1-y, x, z; (vii) x, y, -z; (viii) y, 1-x, 1-z.

Table S2 Selected bond lengths (Å) and angles (º) for **2**.

Cd2—O4^{ii}	2.291(4)	Cd2—O2	2.333(4)
Cd2—O3^{iii}	2.292(4)	Cd2—N1	2.318(4)
Cd2—O1	2.457(4)		
O4^{ii}—Cd2—O3^{iii}	126.52(16)	O4^{ii}—Cd2—N1	92.07(10)
O3^{iii}—Cd2—N1	87.07(11)	N1—Cd2—N1^{iv}	174.1(2)
O4^{ii}—Cd2—O2	86.12(17)	O3^{iii}—Cd2—O2	147.36(17)
N1—Cd2—O2	92.24(11)	O4^{ii}—Cd2—O1	139.44(17)
O3^{iii}—Cd2—O1	94.05(17)	N1—Cd2—O1	89.8(1)
O2—Cd2—O1	53.32(16)	O4^{ii}—Cd2—C1	112.55(19)
O3^{iii}—Cd2—C1	120.94(19)	N1—Cd2—C1	91.15(11)
O2—Cd2—C1	26.43(18)	O1—Cd2—C1	26.89(17)

Symmetry codes: (i) x, y, 2-z; (ii) y, -x+y, 1-z; (iii) 1-y, 1+x-y, z; (iv) x, y, 1-z; (v) -x+y, 1-x, 1-z; (vi) x-y, x, z.

2- Powder X-ray diffraction of MOFs 1-2

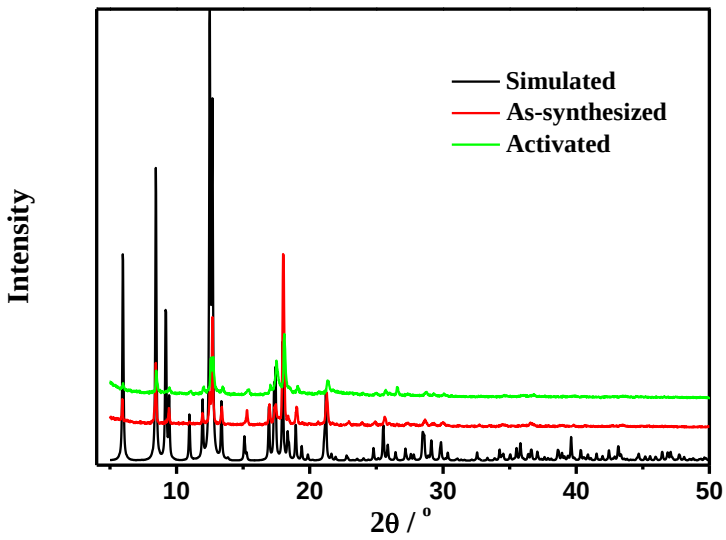

Fig. S1. X-ray powder diffraction patterns of MOF **1**. Note that some differences in intensities between the calculated and experimental patterns may be due to the variation in crystal orientation or framework deterioration in the powdered samples.

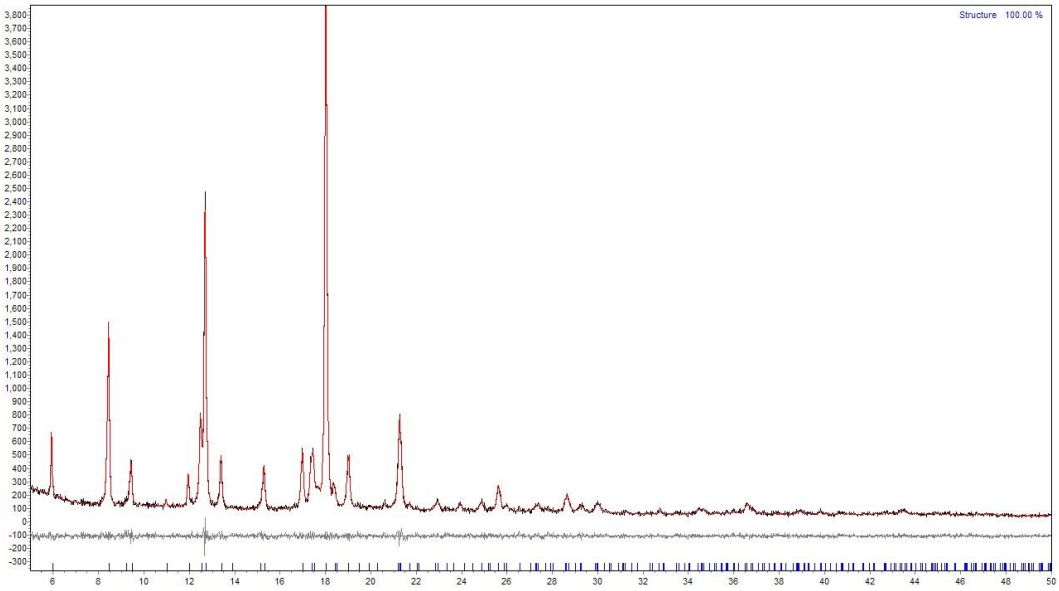

Fig. S2. Profile fitting of X-ray powder diffraction pattern of as-synthesized MOF **1**. The red, blue, and gray lines are the calculated, the as-synthesized and the difference between the calculated and the as-synthesized. The blue bars are the calculated brag positions. The best fitting results for **1**: a = 29.467(6), c = 10.122(3).

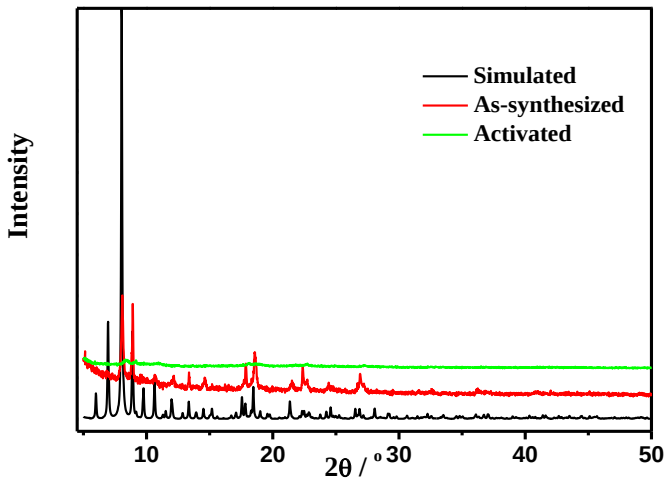

Fig. S3. X -ray powder diffraction patterns of MOF **2**. Note that some differences in intensities between the calculated and experimental patterns may be due to the variation in crystal orientation or framework deterioration in the powdered samples.

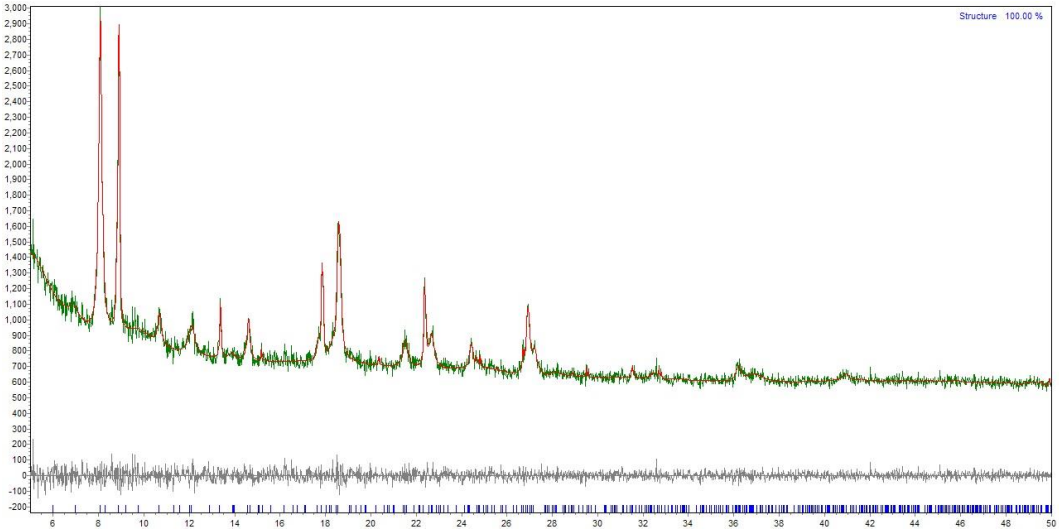

Fig. S4. Profile fitting of X-ray powder diffraction pattern of as-synthesized MOF **2**. The red, black, and gray lines are the calculated, the as-synthesized and the difference between the calculated and the as-synthesized. The blue bars are the calculated brag positions. The best fitting results for **2**: a = 25.321(51), c = 19.911(66).

3- Additional crystallographic figures

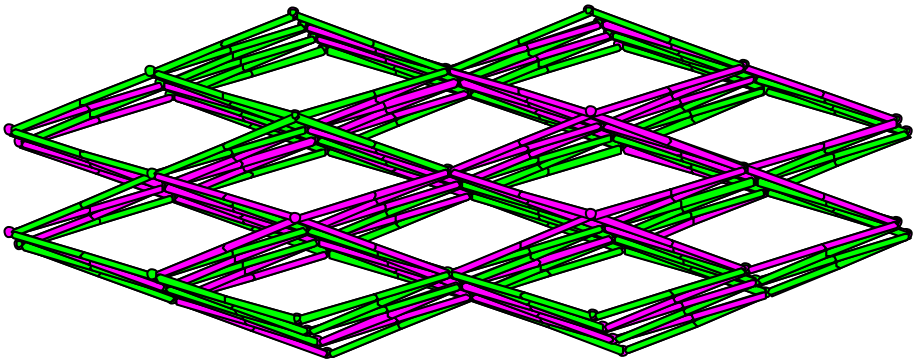

Fig. S5. Simplified doubly-interpenetrating 8-conneted bcu net of MOF **1**.

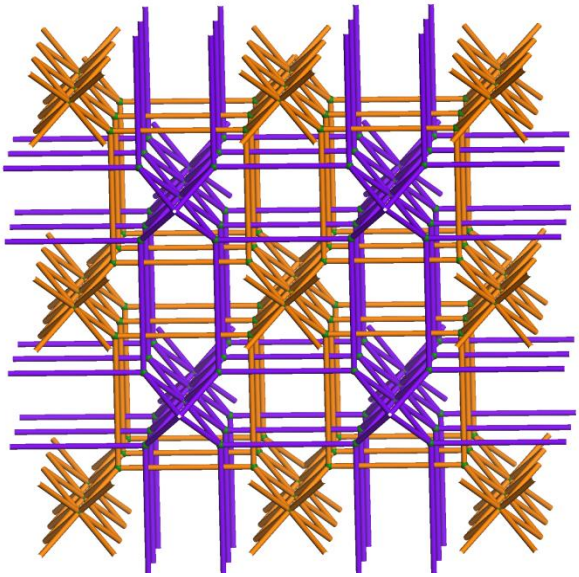

Fig. S6 Simplified doubly-interpenetrating (4,8)-connected sqc928 net of MOF **1**.

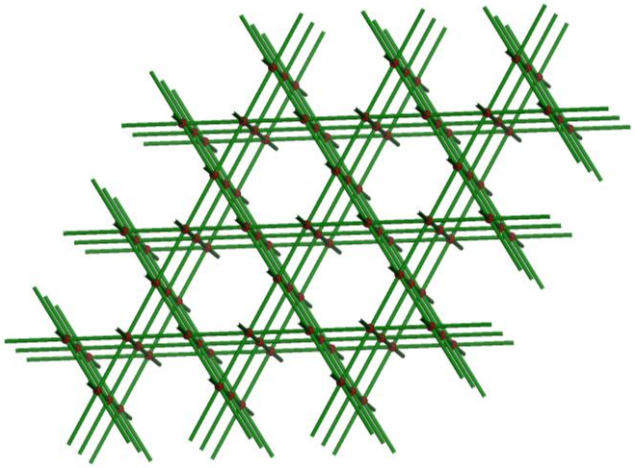

Fig. S7 simplified 6-connected kagome net of **2**.

4- TGA curves for MOFs 1 and 2

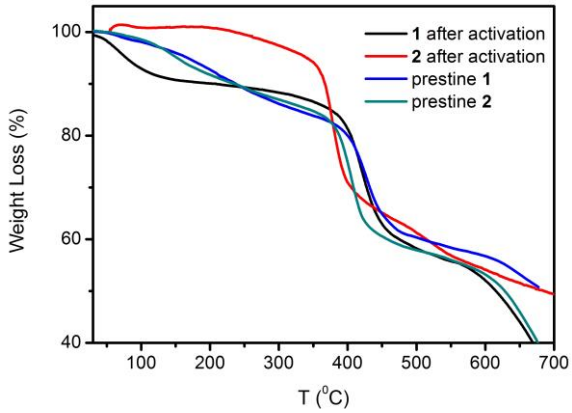

Fig. S8. TGA curves of MOFs **1** and **2**. Note that the activated **1** was left in air for several days before the TGA measurement.

5- Addition gas sorption isotherms for MOF 1.

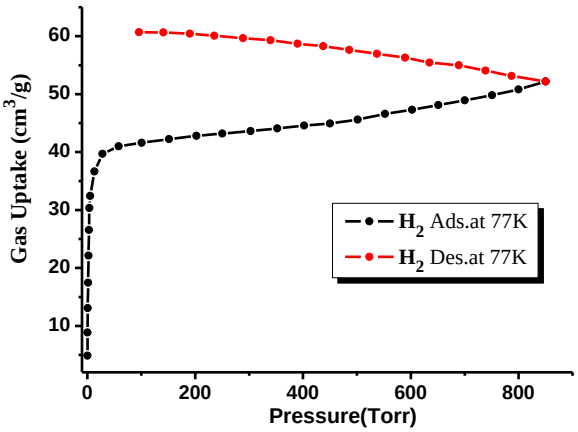

Fig. S9 H_2 gas sorption isotherms of MOF **1** at 77 K.